

**RL-TR-96-273**

**Final Technical Report  
April 1997**



# **VERTICAL CAVITY LASER JOINT STUDY PROGRAM WITH ROME LABORATORY**

**Cornell University**

**William J. Schaff**

**DTIC QUALITY INSPECTED 4**

*APPROVED FOR PUBLIC RELEASE; DISTRIBUTION UNLIMITED.*


**19970605 092**

**Rome Laboratory  
Air Force Materiel Command  
Rome, New York**

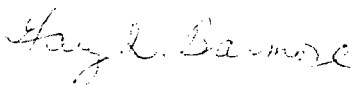
This report has been reviewed by the Rome Laboratory Public Affairs Office (PA) and is releasable to the National Technical Information Service (NTIS). At NTIS it will be releasable to the general public, including foreign nations.

RL-TR-96-273 has been reviewed and is approved for publication.

APPROVED:

  
RICHARD J. MICHALAK  
Project Engineer

FOR THE COMMANDER:

  
GARY D. BARMORE, Maj, USAF  
Deputy Director  
Surveillance & Photonics Directorate

If your address has changed or if you wish to be removed from the Rome Laboratory mailing list, or if the addressee is no longer employed by your organization, please notify RL/OCP, 25 Electronic Pky, Rome, NY 13441-4514. This will assist us in maintaining a current mailing list.

Do not return copies of this report unless contractual obligations or notices on a specific document require that it be returned.

<b>REPORT DOCUMENTATION PAGE</b>			<i>Form Approved</i> OMB No. 0704-0188	
Public reporting burden for this collection of information is estimated to average 1 hour per response, including the time for reviewing instructions, searching existing data sources, gathering and maintaining the data needed, and completing and reviewing the collection of information. Send comments regarding this burden estimate or any other aspect of this collection of information, including suggestions for reducing this burden, to Washington Headquarters Services, Directorate for Information Operations and Reports, 1215 Jefferson Davis Highway, Suite 1204, Arlington, VA 22202-4302, and to the Office of Management and Budget, Paperwork Reduction Project (0704-0188), Washington, DC 20503.				
<b>1. AGENCY USE ONLY (Leave blank)</b>		<b>2. REPORT DATE</b> APR 97	<b>3. REPORT TYPE AND DATES COVERED</b> FINAL, Jul 95 - Jul 96	
<b>4. TITLE AND SUBTITLE</b> VERTICAL CAVITY LASER JOINT STUDY PROGRAM WITH ROME LABORATORY			<b>5. FUNDING NUMBERS</b> C - F30602-95-C-0118 PE - 62702F PR - 4600 TA - P4 WU - PO	
<b>6. AUTHOR(S)</b> William J. Schaff				
<b>7. PERFORMING ORGANIZATION NAME(S) AND ADDRESS(ES)</b> Cornell University Dept of Electrical Engineering 120 Day Hall Ithaca NY 14853			<b>8. PERFORMING ORGANIZATION REPORT NUMBER</b>  N/A	
<b>9. SPONSORING/MONITORING AGENCY NAME(S) AND ADDRESS(ES)</b> Rome Laboratory/OCP 25 Electronic Pky Rome NY 13441-4515			<b>10. SPONSORING/MONITORING AGENCY REPORT NUMBER</b>  RL-TR-96-273	
<b>11. SUPPLEMENTARY NOTES</b> Rome Laboratory Project Engineer: Richard J. Michalak, OCP, (315) 330-3150				
<b>12a. DISTRIBUTION AVAILABILITY STATEMENT</b> Approved for Public Release; Distribution unlimited.			<b>12b. DISTRIBUTION CODE</b>	
<b>13. ABSTRACT (Maximum 200 words)</b> This effort investigated the development of short wavelength VCSEL (vertical cavity surface emitting laser) material for potential application in optical interconnects for radar signal processing subsystems. GaN is the material system used and growth via molecular beam epitaxy on sapphire substrates was extensively investigated. Dry etching studies were performed. Due to the poor quality of these initial growths, VCSELs could not be fabricated.				
<b>14. SUBJECT TERMS</b> gallium nitride, vertical cavity surface emitting lasers (VCSELs), molecular beam epitaxy, optical interconnects, radar signal processing			<b>15. NUMBER OF PAGES</b> 32	
			<b>16. PRICE CODE</b>	
<b>17. SECURITY CLASSIFICATION OF REPORT</b> UNCLASSIFIED	<b>18. SECURITY CLASSIFICATION OF THIS PAGE</b> UNCLASSIFIED	<b>19. SECURITY CLASSIFICATION OF ABSTRACT</b> UNCLASSIFIED	<b>20. LIMITATION OF ABSTRACT</b> UL	

## Final Report

# Vertical Cavity Laser Joint Study Program with Rome Laboratory

William J. Schaff  
School of Electrical Engineering  
Cornell University  
Ithaca, NY 14853

### Abstract

Vertical cavity surface emitting lasers (VCSEL)s have useful properties for optical interconnects and data storage. The topic of this investigation has been fabrication of VCSELs operating at near-UV wavelengths. Short wavelength light emission is possible from GaN semiconductors, and offers smaller diffraction limited spot size than obtained from present materials.

The development of vertical cavity surface emitting lasers (VCSEL)s made from GaN requires greater control of the materials synthesis than presently exists. A central difficulty in this synthesis is the lack of an ideal substrate for epitaxial growth. Most of the effort reported here has focused on the growth of GaN on sapphire substrates by molecular beam epitaxy (MBE), and understanding how lattice mismatched growth has affected the epitaxial layer properties. Samples of GaN for joint dry-etching studies have been supplied to Rome Laboratories. Actual VCSELs could not be fabricated because of inadequate material perfection. The materials development reported here shows significant advancement in understanding the growth of GaN for VCSEL applications and provides good promise for DOD applications.

# Vertical Cavity Laser Joint Study Program with Rome Laboratory

William J. Schaff  
School of Electrical Engineering  
Cornell University  
Ithaca, NY 14853

## Table of Contents

ABSTRACT .....	I
TABLE OF CONTENTS .....	II
LIST OF FIGURES .....	III
BACKGROUND .....	1
GROWTH OF GAN BY MBE .....	2
Remote RF Plasma source of atomic nitrogen.....	3
Sapphire substrate mounting.....	5
Reflection high energy electron diffraction (RHEED).....	8
Atomic force microscopy (AFM).....	11
X-ray diffraction.....	13
Hall effect .....	14
Photoluminescence (PL) .....	16
GROWTH OF INN AND ALGAN BY MBE.....	19
AlGaN PL.....	19
GROWTH OF CUBIC GAN BY MBE .....	20
X-ray of cubic GaN .....	20
SUMMARY .....	21

## List of Figures

FIGURE 1 BANDGAPS FOR WURTZITE AND CUBIC III-NITRIDES .....	1
FIGURE 2 DIAGRAM OF MBE MACHINE USED FOR GROWTH OF III-NITRIDES .....	3
FIGURE 3 OPTICAL SIGNAL CORRESPONDING TO ATOMIC NITROGEN IS SEEN AS A FUNCTION OF RF POWER AND MBE CHAMBER PRESSURE.....	4
FIGURE 4 COMPARISON OF SUBSTRATE THERMOCOUPLE TEMPERATURE AND SUBSTRATE TEMPERATURE MEASURED BY A PYROMETER. ....	5
FIGURE 5 DRAWING THAT SHOWS THE INDIUM FREE METHOD OF MOUNTING THE SAPPHIRE WAFER SLICE FOR GAN GROWTH.....	6
FIGURE 6 ROOM TEMPERATURE MOBILITY OF GAN DOPED AT APPROXIMATELY $1 \times 10^{18} \text{ CM}^{-3}$ AS A FUNCTION OF THERMOCOUPLE TEMPERATURE.....	7
FIGURE 7 RHEED RECONSTRUCTION FOR A SAPPHIRE SUBSTRATE PRIOR TO GROWTH OF GAN. .	8
FIGURE 8 CHANGES IN RHEED PATTERN DURING GROWTH OF GAN ON SAPPHIRE USING 600W RF POWER AND $1.1 \times 10^{-5} \text{ T}$ CHAMBER PRESSURE (WAFER GS0091).....	10
FIGURE 9 ATOMIC FORCE MICROSCOPY (AFM) VIEWS OF GAN GROWN ON SAPPHIRE .....	12
FIGURE 10 X-RAY DIFFRACTION PATTERNS COMPARING A SAPPHIRE SUBSTRATE AND GAN GROWN ON TOP. THE CENTER LOCATIONS HAVE BEEN ADJUSTED FOR OVERLAP.....	13
FIGURE 11 ROOM TEMPERATURE HALL MOBILITIES AS A FUNCTION OF CARRIER CONCENTRATION FOR N-TYPE WURTZITE GAN GROWN IN DIFFERENT LABORATORIES .....	14
FIGURE 12 CARRIER CONCENTRATION IN N-TYPE GAN AS A FUNCTION OF RECIPROCAL TEMPERATURE OF THE SI DOPING FURNACE.....	15
FIGURE 13 ROOM TEMPERATURE PHOTOLUMINESCENCE OF GAN AS A FUNCTION OF N-TYPE DOPING CONCENTRATION.....	17
FIGURE 14 MODEL OF BAND DIAGRAM SURROUNDING VERTICALLY ORIENTED DEFECT IN GAN WHICH SHOWS FERMI-LEVEL PINNING AT THE DEFECT LEVEL AND BAND BENDING AWAY FROM THE DEFECT. ....	18
FIGURE 15 MODEL OF DEFECT LEVEL IN THE PRESENCE OF TWO DIFFERENT DOPING CONCENTRATIONS ILLUSTRATING DIFFERENT DEPLETION REGIONS SURROUNDING THE DEFECT. ....	18
FIGURE 16 ROOM TEMPERATURE PL FROM UNDOPED ALGAN FOR TWO DIFFERENT COMPOSITIONS. NO BAND EDGE LUMINESCENCE IS SEEN (THE HIGH ENERGY SIGNAL IS FROM THE UV LASER).....	20
FIGURE 17 X-RAY DIFFRACTION OF $0.2 \mu\text{M}$ THICK CUBIC GAN GROWN ON SIC AT CORNELL AT 600W RF POWER.....	21

## Background

The future packing density of optical interconnects will require shorter wavelength lasers than presently exist. Optical storage will similarly benefit from smaller diffraction limited spot sizes at shorter wavelengths. The only direct bandgap semiconductors which can emit light in the UV wavelength regions are the III-nitrides; GaN and compounds of AlGaN. A diagram showing the bandgap (and therefore emission wavelength) dependence of the III-nitrides as a function of lattice constant is shown in Figure 1.

Two different forms of GaN, AlN and InN can exist. They are Wurtzite (hexagonal) structures, or they can exist as cubic forms. The most common forms of these materials are the Wurtzite structures. Cubic nitrides are more difficult to synthesize as a practical matter because lattice matched cubic substrates do not exist. It can be seen that the bandgap of hexagonal GaN corresponds to a wavelength of approximately 380nm in the UV. Alloys of AlGaN move the bandgap to higher energies where emission wavelengths closer to 300nm appear possible.

There is a significant difference in the manner of change in bandgaps of the III-nitrides compared to the more conventional III-arsenide semiconductors. AlN is significantly lattice mismatched to GaN while AlAs is nearly lattice matched to GaAs. As a result, it is not possible to grow very thick clad layers of AlN on GaN without generating lattice defects to accommodate the difference in lattice constants. It is very difficult to make lateral cavity lasers with sufficient optical confinement for good efficiency when constrained to the thicknesses presented in the AlGaN materials system.

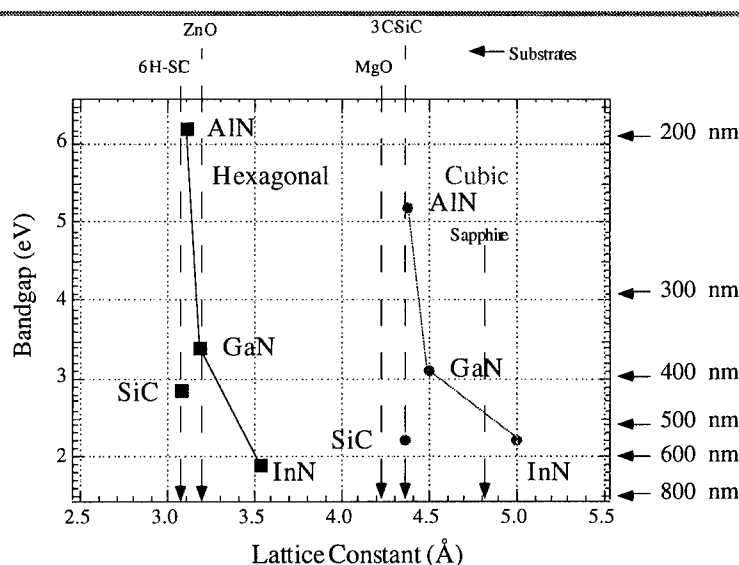


Figure 1 Bandgaps for Wurtzite and cubic III-nitrides

VCSELs do not require the same single thick clad layer that lateral lasers use. Instead, mirrors of multiple layers of two different compositions are required. Strained layer superlattices can be fabricated below critical thickness for GaN based VCSELs. As a result, this study has chosen the VCSEL structure for short wavelength applications.

## **Growth of GaN by MBE**

All GaN materials grown for this program came from a molecular beam epitaxy (MBE) machine which has been configured during this study for growth of nitrides. A schematic of the MBE machine is seen in Figure 2. Conventional thermal sources are used for the group III elements and dopants. Nitrogen gas cannot be directly used for GaN growth. Nitrogen ( $N_2$ ) must be dissociated prior to reaching the surface of the substrate in order to incorporate in GaN. The technique used in this program to break the nitrogen molecule was the application of 13.6 MHz RF energy to form a nitrogen plasma in an atomic nitrogen source assembly which has an opening that faces the substrate. A fraction of approximately 6-8% of the gas which enters the remote RF plasma source will exit as atomic nitrogen. The plasma source is an Oxford Instruments model Cars-25.

The majority of nitrogen will enter the chamber as  $N_2$ . Since it cannot be used for growth of GaN, it must be rapidly removed to avoid degrading the desired growth process. A 2400 l/sec turbomolecular pump efficiently removes unreacted  $N_2$  from the chamber and keeps the pressure in the range of low  $10^{-5}$ T while  $N_2$  is flowing in at a rate of 2-3 sccm. The drawbacks to using a turbomolecular pump include oil backstreaming from oil-based roughing pumps, and the possibility of catastrophic failure of internal seals which can rupture and fill the chamber with pump oil. This mode of failure did occur during the process of this program. The problem was repaired and no contamination of GaAs films was subsequently detected. It is presumed that GaN was similarly unaffected by the failure, but the possibility remains that the results of this study have been affected in ways that were not evident at the time when the program ended.



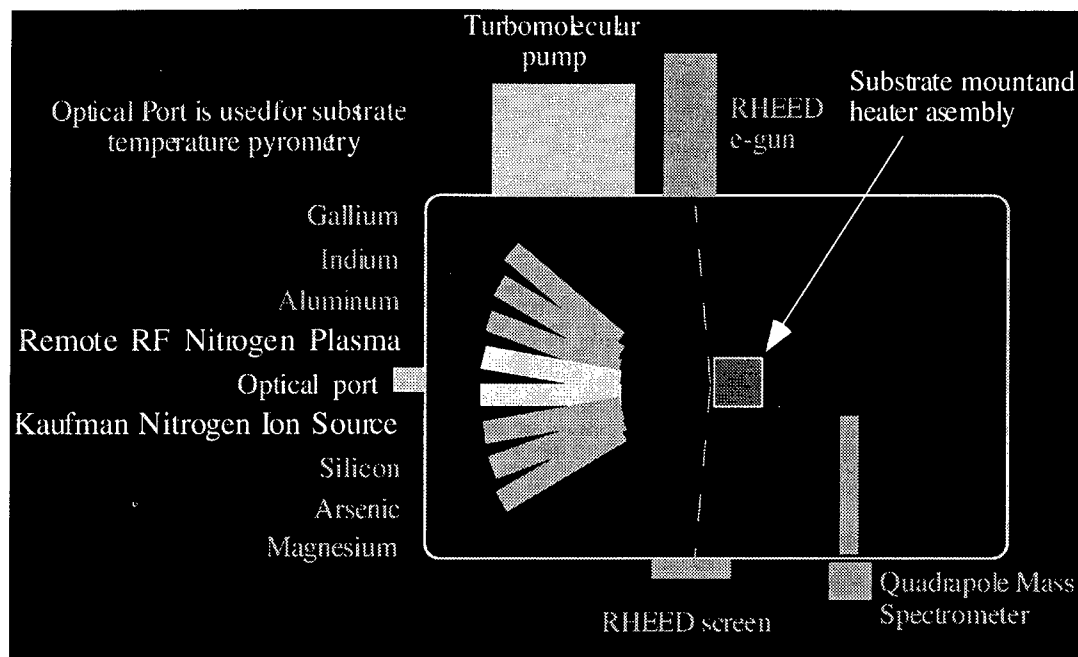


**Figure 2 Diagram of MBE machine used for growth of III-nitrides**

An additional concern when employing source gas in a MBE machine is the possibility of contamination of the growth environment through source gas impurities. Oxygen is normally to be avoided to the greatest possible extent in MBE growth of semiconductors. The starting point for high purity nitrogen gas used in this facility is employment of boil-off gas from a liquid nitrogen tank as a nitrogen source. This is one of the highest purity starting gases available. Following standard ultra-high purity practices, the gas enters the MBE gas cabinet where it is further purified through the use of commercial resin filters. An additional point of use resin filter is used just before gas enters the RF plasma source.

The Kaufman ion source seen in Figure 2 has not been used in this effort. It will be used in future studies of the growth of GaN. The Mg and Si dopants will be discussed later in this report.

### **Remote RF Plasma source of atomic nitrogen**

Atomic nitrogen present in the source can be monitored through the observation of the optical spectrum of the plasma glow. Optical filters to reject all wavelengths of light except those that come from atomic nitrogen transition lines are used in front of an optical detector. The detector output is directly proportional to the amount of atomic nitrogen present in the plasma. The atomic nitrogen signal is dependent on RF power and the amount of nitrogen that is injected into the

source. A plot of the atomic nitrogen signal as a function of power and amount of nitrogen (measured as MBE chamber pressure) is seen in Figure 3.

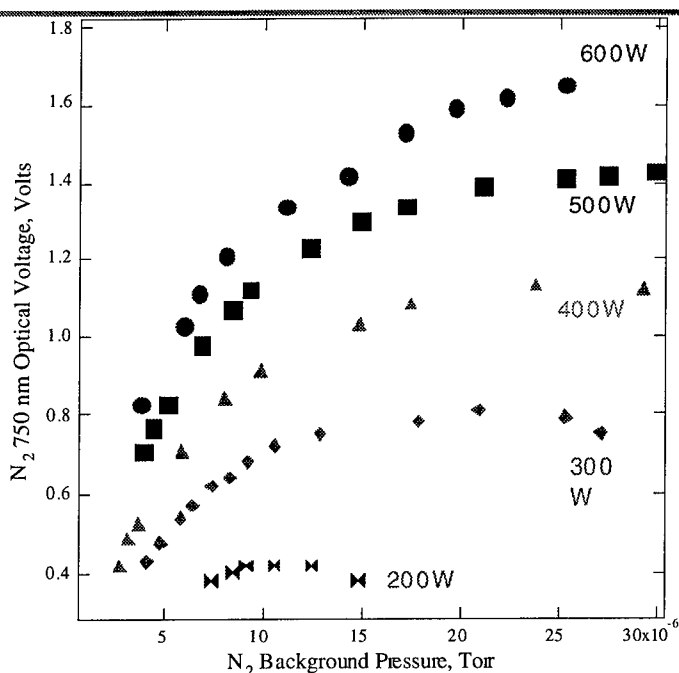


**Figure 3 Optical signal corresponding to atomic nitrogen is seen as a function of RF power and MBE chamber pressure.**

The curve does not show the limited range in pressure over which a plasma can be struck, or ignited, at each power level. The plasma will only turn on within a narrow band of pressure somewhere within the center of each curve shown. The band is widest for highest RF power and narrower for low power. If the plasma is operated outside of this strike range and should go out, it will not restart without intervention to change pressure back to the strike range.

Another aspect of plasma operation is source temperature. The source is designed to be cooled by a large flow of

cold  $N_2$  gas. The source of gas is  $LN_2$  which is warmed through a heating coil to enter the source at a temperature of approximately  $-20^\circ C$ . The amount of  $LN_2$  consumed dictates that the source must be fed from a large outdoor tank to be operational for periods on the order of a day or more without interruption. In practice, it is very difficult to regulate the flow of nitrogen gas to the source because the vacuum jacketed delivery system is shared by the  $LN_2$  phase separator used to cool the MBE machine. The pressure variations in this system are so great that a solenoid in the gas line to the RF source must be controlled by a thermocouple in the source. Although this system works for the majority of conditions encountered, there are times when pressure transients cause the source to become too hot for safe operation, or so cold that the plasma is extinguished. Between 25 and 50% of all growth starts were ruined when the plasma went out. Some improvement could be seen by being careful to keep the plasma pressure within the strike range, but reliable operation remains a topic of development. For this reason, this commercial plasma source would not be recommended for new programs involving the MBE growth of GaN unless drastic measures are taken to solidify plasma stability.

## Sapphire substrate mounting

Sapphire was used almost exclusively as the substrate for GaN growth for this study. For the first 9 months of the program, sapphire was mounted to molybdenum ("moly") substrate blocks using indium as a solder. This is the technique which had been employed for almost 20 years for mounting small substrates for MBE growth. Sapphire was prepared in three different configurations for these growths. A one inch substrate would be used whole, or cut in half, while 2 inch substrates were cut into quarters and only a quarter would be used at a time. These smaller pieces were used to minimize substrate costs. These smaller pieces would then be mounted to the moly block with indium in the same fashion as used previously for GaAs.

The excellent thermal contact offered by indium solder has been helpful towards minimizing one problem in the control of substrate temperature in MBE. The substrate is very close in temperature to the temperature of the moly block. This helps to identify the actual temperature of the substrate itself. The block is not in direct contact with the substrate heater station thermocouple. The thermocouple is radiatively heated by the back of the moly block. Unfortunately, the thermocouple receives some heat from the heater filaments which raises the thermocouple temperature above that of the moly block. A comparison between the thermocouple temperature and the moly block

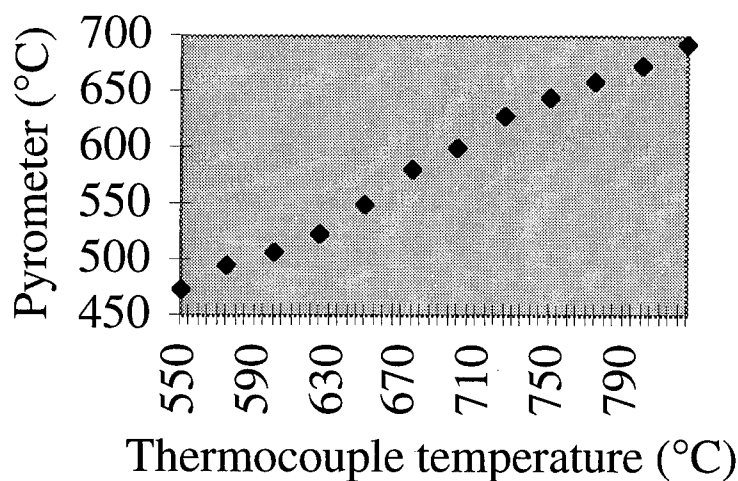


Figure 4 Comparison of substrate thermocouple temperature and substrate temperature measured by a pyrometer.

/substrate temperature measured by a pyrometer is seen in Figure 4. It can be seen that the thermocouple temperature is approximately 200°C hotter than the actual substrate temperature. Although all reports of temperature in this effort are those measured by the thermocouple, it can be seen that actual temperatures are lower. The difference between the actual and the control temperature can vary widely between different laboratories. These differences make it difficult to utilize

conditions reported by other labs without undergoing the expensive process of formulating parameter variation curves to establish similar relationships.

Although indium mounting provides excellent heat transfer from the moly block to the substrate, it has a disadvantage for the growth of GaN that is often not seen for GaAs growths. GaN grows at slow growth rates ( $0.1\mu\text{m}$  to  $0.2\mu\text{m}$  per hour) compared to GaAs ( $1.0\mu\text{m}$  per hour). As a result, typical growths take 5 to 10 times longer - sometimes lasting for more than one day. During these long times, the substrate is held at temperatures of approximately  $700^{\circ}\text{C}$  and an initial substrate nitridization occurs at approximately  $800^{\circ}\text{C}$ . At these long times and high temperatures, significantly more indium solder evaporates away from between the substrate and moly block than occurs for GaAs. The effects of this evaporation are very harmful to GaN growth.

When indium evaporates, the thermal contact between the moly block and substrates becomes

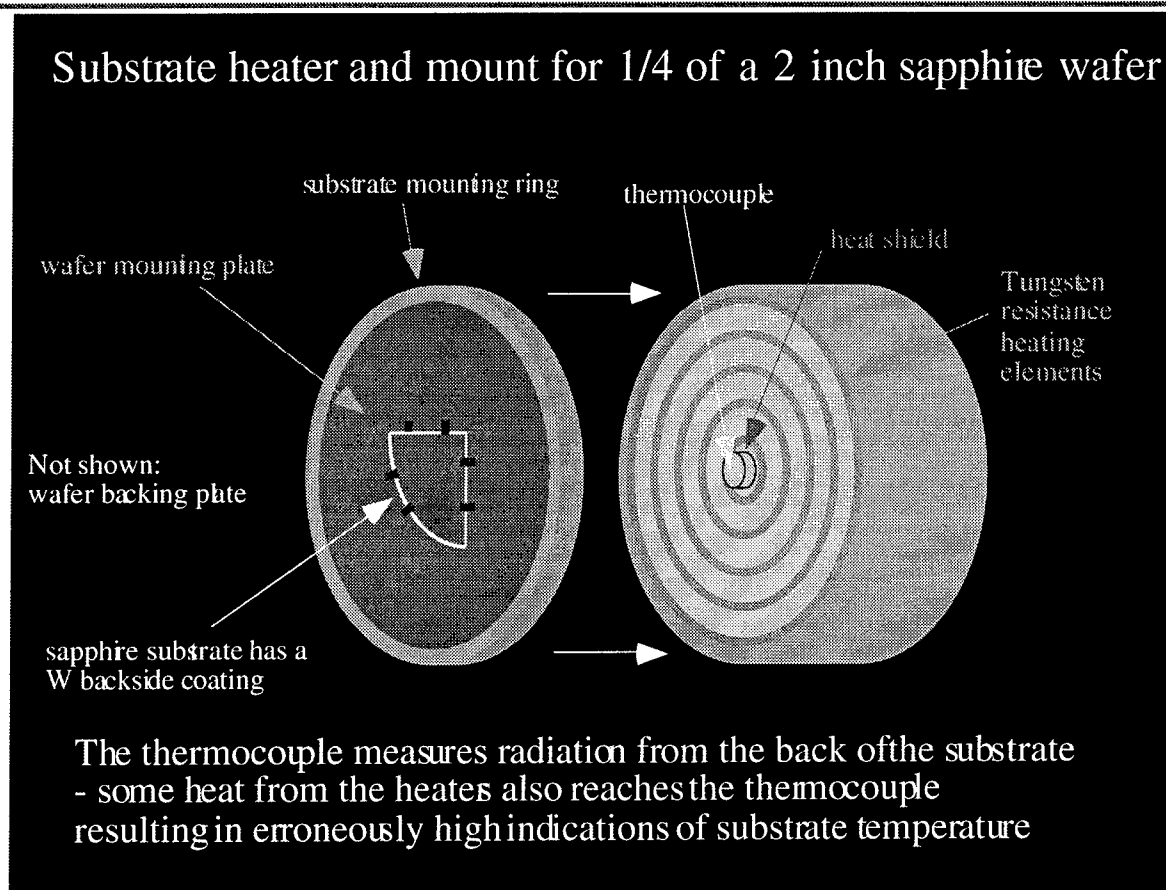


Figure 5 Drawing that shows the indium free method of mounting the sapphire wafer slice for GaN growth.

---

smaller and the substrate surface temperature falls while the moly block temperature is held constant by the control thermocouple. Substrate temperature is an important parameter in controlling the quality of GaN as shown later in this report. As a result of falling substrate temperature, the growth conditions change so much during a long growth that the material quality varies with depth and is poorest at the surface. It becomes very difficult to develop techniques to optimize material quality under these conditions. In addition, approximately one wafer out of every four grown will fall off of the moly block because too much indium solder evaporates.

These difficulties took several months to uncover, however the solution which was reached has been very valuable to reproducibility of GaN growth. The new method of mounting substrates is seen in Figure 5. The wafer is held by clips between a backing plate and front plate. The backing plate has a cutout of the same shape and size as the substrate. This permits heat from the heaters to directly radiate onto the substrate.

The new substrate mounting technique presents a new problem. The blackbody radiation from the heaters largely passes through the transparent sapphire substrate. In order to raise the actual substrate temperature to a given value, the heaters must be set to much higher power than was used for the indium substrate mounting. This is

undesirable for a number of reasons. The higher power will produce more outgassing of unintentional background gases from the hotter substrate heater mechanism. These gases can

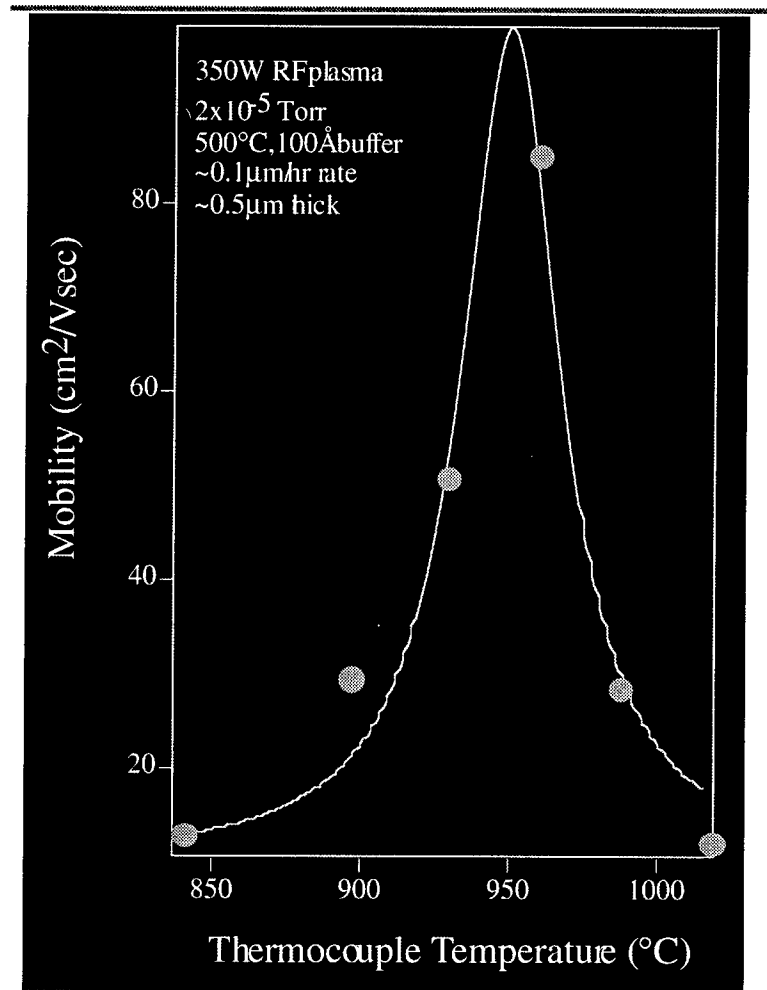


Figure 6 Room temperature mobility of GaN doped at approximately  $1 \times 10^{18} \text{ cm}^{-3}$  as a function of thermocouple temperature.

contaminate the purity of the growing GaN wafer. The higher power will also shorten the lifetime of the substrate heater filament, and will establish a smaller upper limit to maximum substrate temperatures that can be reached. For these reasons, the substrates are metallized with tungsten, and prepared with roughened backsides to increase radiative heat absorption. If the substrate is not roughened prior to metallization, the metal will resemble a mirror and reflect significant amounts of heat back to the heaters rather than transfer the heat to the substrate. Using this technique, it is possible to obtain pyrometer measurements of substrate temperature that are very close to those of indium bonded substrates.

Most of the wafers for this program were grown before the change to non-indium bonded substrates. In another program, a new calibration of GaN wafer properties as a function of substrate temperature was performed. One of the most important properties of GaN for application to VCSELs is mobility. High mobilities are desired to permit low resistance electrical conduction between ohmic contacts and the laser active region.

#### **Reflection high energy electron diffraction (RHEED)**

An important element of GaN growth by MBE is the ability to monitor the growing surface using reflection high energy electron diffraction (RHEED). The RHEED reconstruction seen on a phosphor screen can give indications about the relative quality of the growing surface. It has been

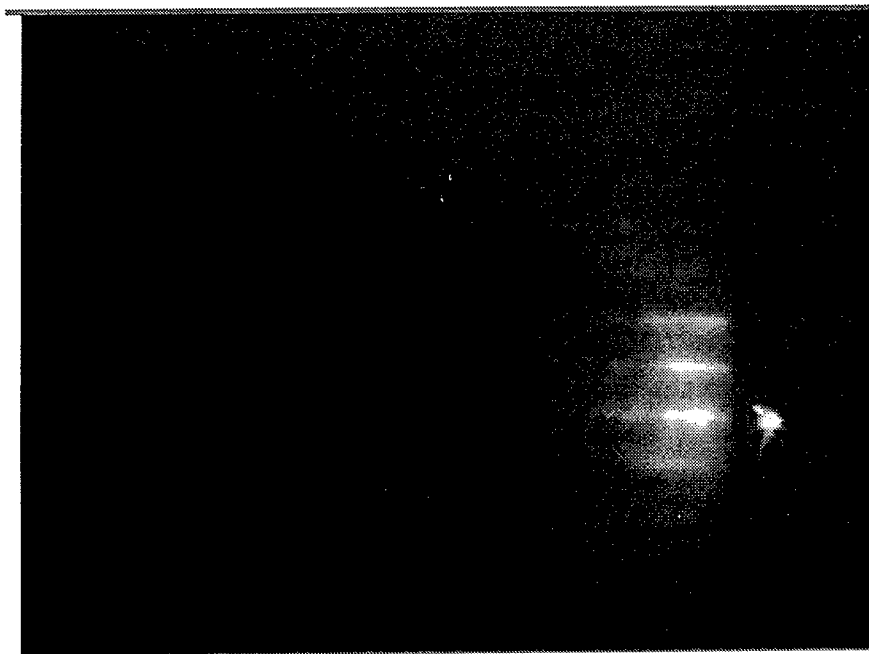


Figure 7 RHEED reconstruction for a sapphire substrate prior to growth of GaN.

useful to identify the type of GaN crystal lattice also. It is clear from RHEED when GaN is a Wurtzite form, or a cubic form. Some cubic GaN was grown for this program on cubic SiC which clearly showed cubic symmetry. When GaN was grown on GaAs, the RHEED pattern did not show only cubic symmetry, but instead a combination of cubic and Wurtzite phases were observed. This is an important observation because X-Ray diffraction of GaN grown on GaAs often is more sensitive to the cubic phase of the material and has lead to many false reports of cubic GaN on GaAs.

RHEED observations of GaN growth begin with observation of the sapphire substrate. The RHEED reconstruction from a typical sapphire substrate is seen in Figure 7. The horizontal lines indicate that the surface consists of a regular pattern of atoms. The RHEED reconstruction can be thought of in terms of the reciprocal of the surface atom arrangement. A regular flat array of atoms will be transformed in appearance to an array of lines while a non-flat array will give rise to spots. A spotty RHEED pattern indicates that there is surface roughness on more than an atomic scale. A crystal that grows under this condition for extended thicknesses will likely exhibit defects in crystalline perfection which will be observed with X-Ray diffraction, or electrical and optical properties.

Roughened surfaces with increased layer thicknesses are often seen for lattice mismatched growth. Rough surfaces have been seen in most GaN growth performed under this program. Typical RHEED reconstruction at different points in the growth of GaN is seen in Figure 8.

Growth initially remains flat as a thin buffer is grown at low temperatures. The low temperature layer is necessary to initiate nucleation. If higher thermocouple temperatures, such as 800°C are used to grow on the bare substrate, no growth will take place, even after several hours of exposure to Ga and atomic nitrogen. Not shown is the RHEED pattern during this initial 700°C growth. It would show that the surface appears to be amorphous after approximately 5-10 monolayers (ML)s. When the growth is interrupted for 2 minutes, the pattern anneals to the form seen in Figure 8. With this very thin layer of growth, the surface seems to be planar and regular. It becomes apparent with further growth that the surface becomes rough and somewhat irregular. After just a limited amount of additional growth, the RHEED pattern becomes spotty and remains this way for any thickness which follows. The spotty growth is presumed to result from rough surfaces caused by the lattice mismatched growth.

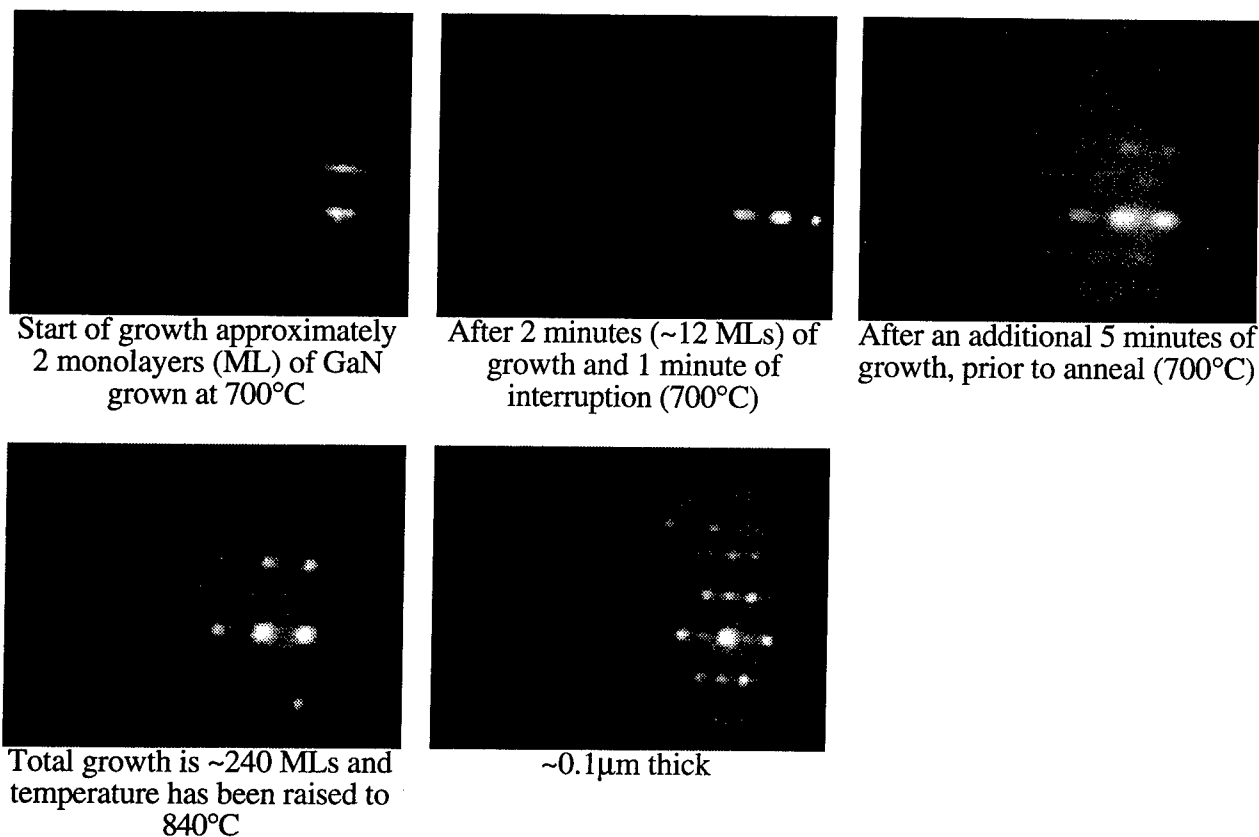


**Figure 8 Changes in RHEED pattern during growth of GaN on sapphire using 600W RF power and  $1.1 \times 10^{-5}$  T chamber pressure (wafer GS0091)**

This rough surface growth is almost always seen. The exception is when growth conditions are selected which provide insufficient nitrogen overpressure for stoichiometric growth. When the Ga flux is raised to too high of a growth rate, excellent RHEED patterns are seen. The RHEED is streaky and bright which would seem to indicate very good crystal quality. The films, however show large densities of Ga droplets all over the surface. It is not hard to understand how insufficient nitrogen would lead to Ga droplets - excess Ga atoms that migrate on the growing surface would migrate into balls which would continue to grow. It is difficult to understand why the RHEED pattern would look so good. Presumably it indicates that the small GaN islands between the Ga droplets might be of very good quality. There may be some 3D growth taking place free of lattice mismatch dislocations. If so, some form of control of this condition might lead to a better quality crystal. GaN grown with insufficient nitrogen also usually has much stronger photoluminescence quality than films grown without Ga droplets. This characteristic would be desirable for laser application. The density of the droplets, however, is much too high to permit laser device fabrication.



## Atomic force microscopy (AFM)

Early efforts to establish suitable growth conditions for GaN made extensive use of atomic force microscopy (AFM). This technique helped identify useful initial substrate nitriding conditions and buffer growth conditions. It was found through AFM observations that an optimum substrate nitriding condition prior to growth was 3 minutes exposure to atomic nitrogen at 1050°C. Following this step, optimum buffers were established using AFM. Substrate thermocouple temperatures of 700°C permitted nucleation of GaN, while higher temperatures did not.

Some AFM images from early growths are seen in Figure 9. In the top image, the white areas are Ga droplets which are higher than the surface of the GaN. At higher magnification in the image at the bottom, islands of GaN are seen at this early stage of growth. In some areas the boundaries of the islands can be seen. These boundaries that appear are the interface defects which exist between the early GaN island nucleation and continue to exist throughout the entire vertical layer growth of an observed thickness. The electrical and optical properties of these defects are discussed later in this report.

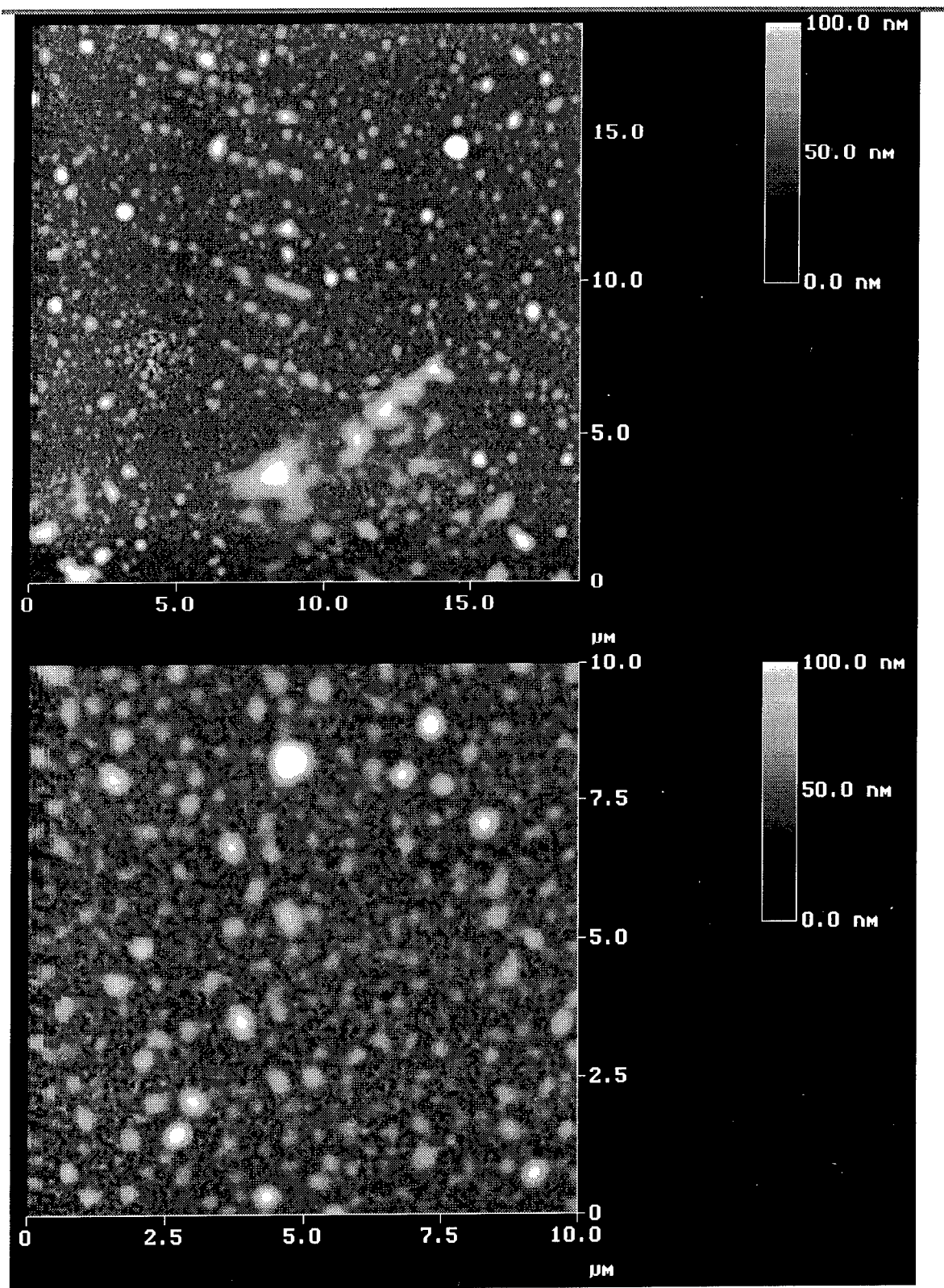


Figure 9 Atomic force microscopy (AFM) views of GaN grown on sapphire

## X-ray diffraction

X-ray diffraction of GaN is employed to determine the effect of growth conditions on the crystallinity of the grown film. A composite of typical x-ray diffraction patterns is seen in Figure 10. The full width half maximum for GaN far exceeds the sapphire substrate. Even though the x-ray indicates that the GaN is essentially a single crystal, the large diffraction width shows that the crystal is rich in defects resulting from the lattice mismatch with the sapphire substrate. While x-ray widths from some growths are better than that shown here, none are comparable to lattice matched epitaxy to good quality substrates in other materials systems.

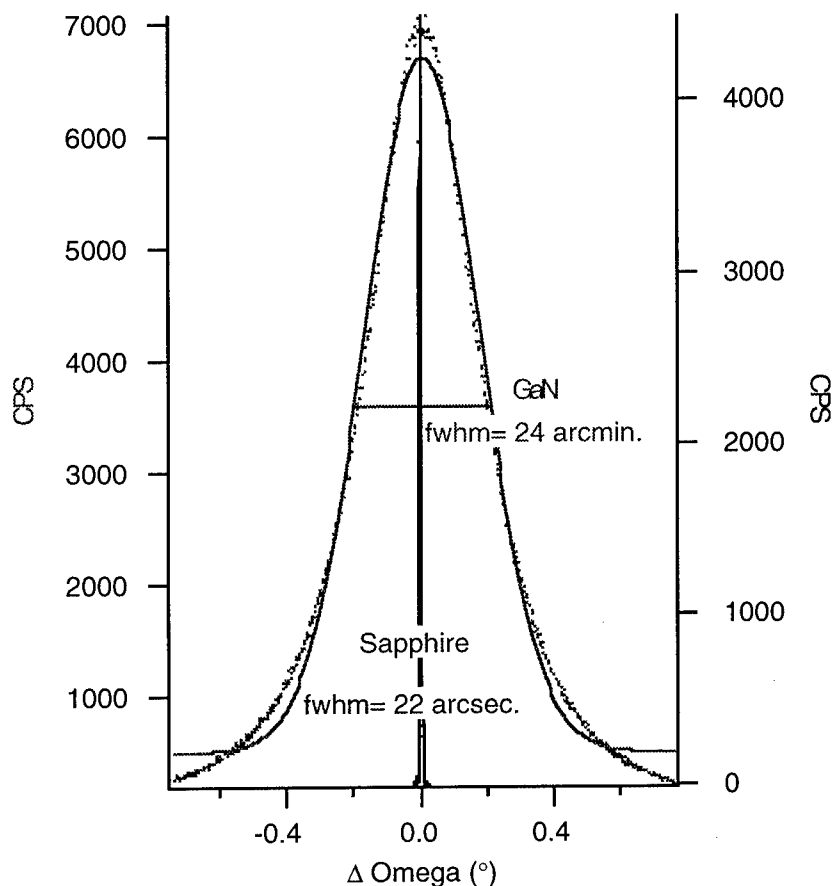


Figure 10 X-ray diffraction patterns comparing a sapphire substrate and GaN grown on top. The center locations have been adjusted for overlap.

## Hall effect

The electrical properties of GaN need to be optimized for application to lasers. High conductivity is desired for low parasitic resistances in the laser diode. Conductivity is proportional to the product of Hall mobility and carrier concentration. Therefore, one goal for GaN used in laser applications is to obtain the highest possible doping concentrations at the highest Hall mobilities possible. The majority of GaN wafer growths made for this program were designed to study the effect of growth conditions on carrier mobility. Some early mobilities for n-type GaN obtained at Cornell under this, and a NSF program, and results from elsewhere are seen in Figure 11.

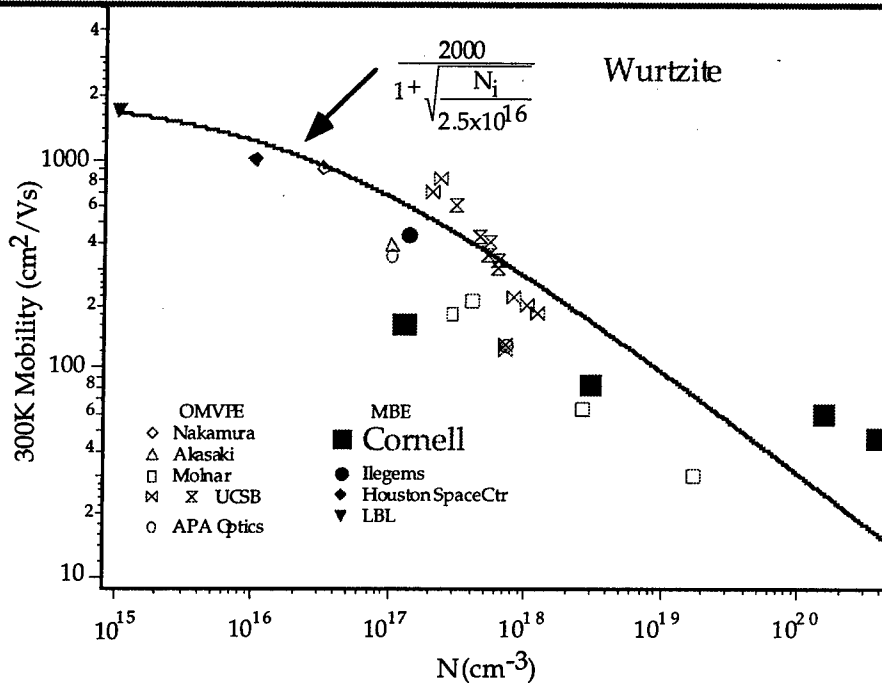


Figure 11 Room temperature Hall mobilities as a function of carrier concentration for n-type Wurtzite GaN grown in different laboratories

The mobilities follow an inverse square root relationship with doping (carrier) concentration typical of other semiconductors. Mobilities are very high for the highest doped GaN grown at Cornell. These samples doped beyond  $1 \times 10^{20} \text{ cm}^{-3}$  have the highest conductivity reported in GaN to date. Although the mobilities are approximately 20-40 times lower than those for highly doped GaAs, the doping concentrations are significantly higher than those that can be obtained in GaAs. The product of doping and mobility is therefore slightly higher for GaN than for GaAs. This material should produce very low parasitic resistances in laser applications.

The mobilities obtained at Cornell at lower doping concentrations are lower than reported in other labs and are a matter of concern. The low mobilities are thought to result from our choice of relatively thin structures for evaluation of doping and mobility studies. The data from this program shown above are from layers that are 1 micron thick. It is known that mobility in GaN gets higher as thicker layers are grown. Presumably this is the result of defects associated with lattice

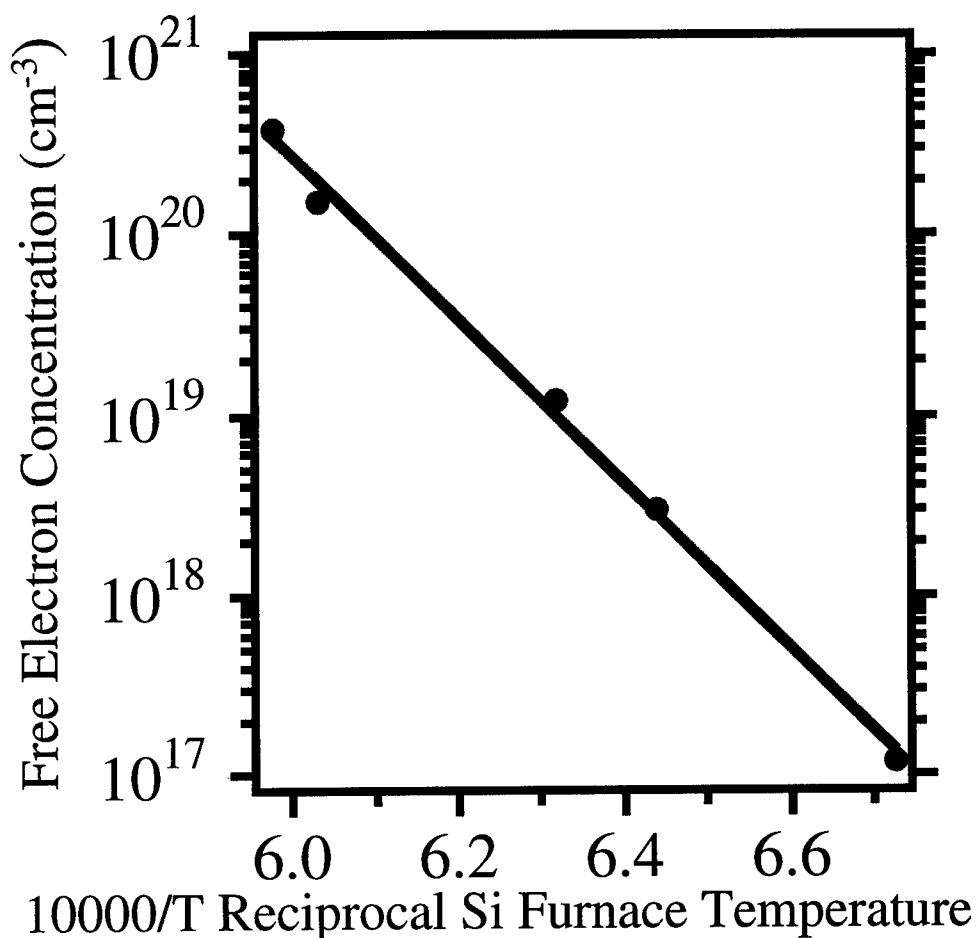


Figure 12 Carrier concentration in n-type GaN as a function of reciprocal temperature of the Si doping furnace

mismatched growth which are greatest in density near the substrate. A single attempt to grow a thicker layer of 3 microns did not have significantly higher mobility than the 1 micron thick reference. It is not known whether this result is a single anomaly, or is representative of all thicker layers. It is the only thick wafer growth attempted under this program.

Another possible explanation for unexpectedly low mobility is scattering from impurities or defects. It is unlikely that ionized impurities exist in significant concentration for these wafers.

Shown in Figure 12 is the Si doping calibration data for GaN obtained for 600W plasma power and 0.1  $\mu\text{m}/\text{hour}$  growth rate. The curve contains two interesting features. First the curve is linear over a wide range, including at lower doping concentrations. This would not be the case if there were a significant concentration of undoped impurities. In addition, undoped material has higher resistivity and does not exhibit significant concentrations of ionized impurities. Thus, large compensation densities as a cause of low mobility is unlikely. Second the very high doping concentrations that are shown are surprising in this wide bandgap semiconductor. These levels are usually only seen in small bandgap semiconductors, and not even materials such as GaAs exhibit such good doping behavior.

In contrast to the n-type doping, p doping has proved to be more troublesome. Although a p-type doping curve for Mg in GaAs has been established during this study, it cannot be sure that the few p-type data points for GaN are unambiguous. P-doping of GaN remains a difficult problem which must be solved for fabrication of VCSELs. Present lateral GaN lasers suffer significant IR drops due to poor p-type GaN doping concentrations.

### **Photoluminescence (PL)**

Photoluminescence (PL) is an important technique for evaluation of the radiative recombination efficiency of GaN. It has also been used in this study to formulate a model to explain the role of defects arising from lattice mismatched growth.

PL from GaN grown at 600W RF plasma power,  $2 \times 10^{-5}\text{T}$  chamber nitrogen pressure,  $840^\circ\text{C}$  substrate temperature (using indium bonded samples) and Si doped to the levels indicated, is shown in Figure 13. The incident laser intensity is very low compared to PL commonly performed on semiconductors. The 20mW laser power is spread over a beam width of approximately 5mm diameter at the surface of the sample. This corresponds to a power density of approximately  $.01\text{W}/\text{cm}^2$ . Most PL of semiconductors is performed at much higher power densities.

The low incident power density provides an opportunity to closely examine PL from deep centers within GaN. Since these centers would be expected to saturate and leave only observation of the bound exciton at the band edge at high power densities, low excitation power density permits easy observation of the relationship between deep level filling and band edge luminescence.

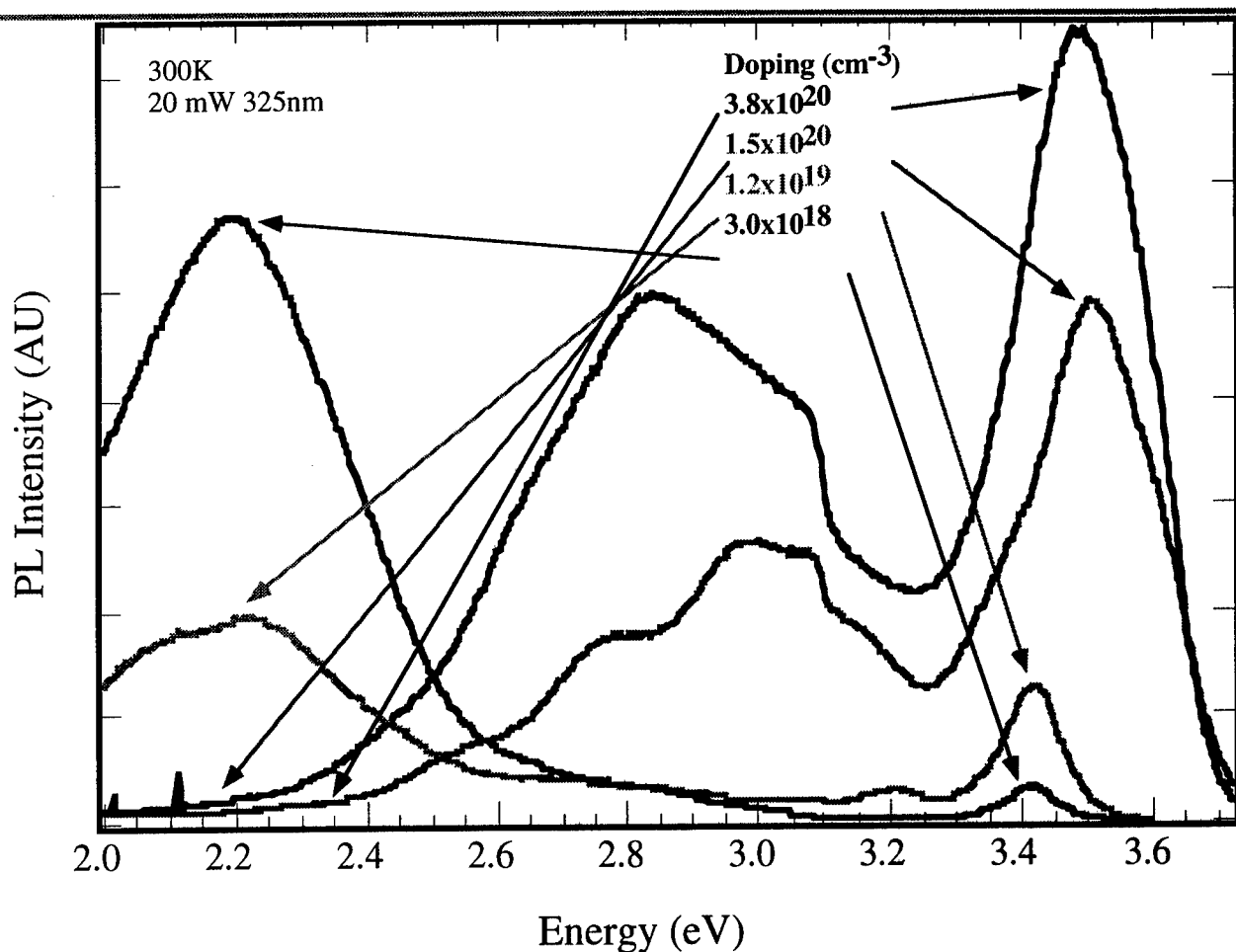
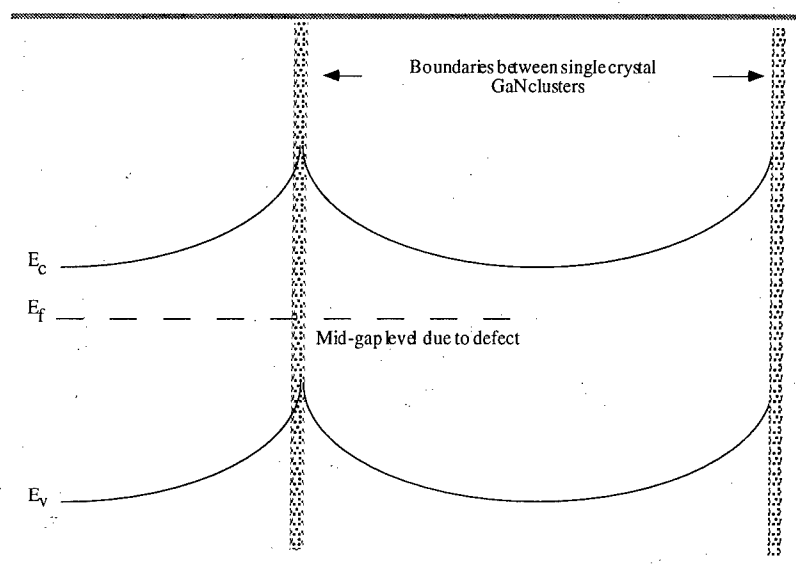


Figure 13 Room temperature photoluminescence of GaN as a function of n-type doping concentration.

It can be seen that at low doping concentrations, luminescence at yellow wavelengths dominates the PL spectra. Not shown is undoped GaN which has only yellow luminescence and no band edge features at 3.4 eV. As doping concentration is raised, the yellow luminescence falls and band edge luminescence rises. Increased band edge PL with increased doping is not unexpected as the electrons provided by the donors increase the probability of recombination with free holes generated by the incident photons. The decrease in deep level luminescence is not expected for increased doping.

Decreased recombination from the deep level at increased doping concentration can be explained by a model proposed by the investigator of this study. The deep level is modeled to be 2.2eV above the valence band of GaN. The deep level luminescence is from the transition from the deep level to

the valence band. The physical origin of the deep level is presumed to be from defects arising from lattice mismatch. These defects are often seen to rise perpendicularly from the substrate interface to the surface. A cross section might appear as simple vertical lines. A schematic showing the band diagram as a function of position is seen in Figure 14.



The defect level pins the Fermi-level near mid-gap. The area surrounding the defect is depleted of carriers. If the combination of low doping density and high defect density exists, the material will exhibit very high resistivity. The undoped samples that we have grown at 600W do exhibit high resistivity.

Figure 14 Model of band diagram surrounding vertically oriented defect in GaN which shows Fermi-level pinning at the defect level and band bending away from the defect.

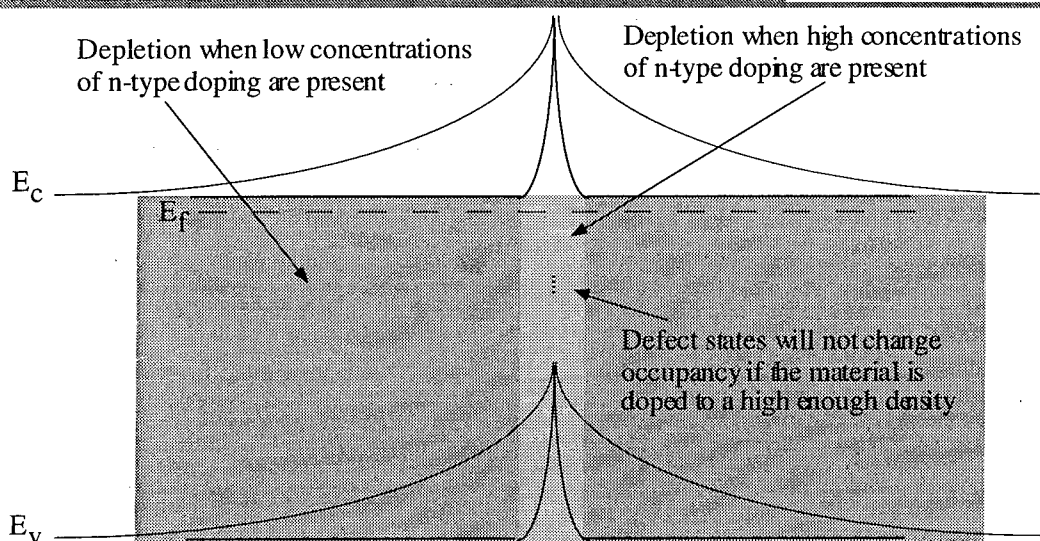


Figure 15 Model of defect level in the presence of two different doping concentrations illustrating different depletion regions surrounding the defect.



Figure 15 shows the effect of doping on the depletion regions surrounding the defect. Higher doping will result in a much greater fraction of material which is "flat-band" and much less material will be depleted surrounding the defect. The probability of band edge luminescence will be highest for the highest doped material, and the probability of luminescence from the defect will be lowest. In addition, the highest doped material will move the Fermi-level above the defect level where it will be completely occupied.

## **Growth of InN and AlGaN by MBE**

Both AlGaN and InN were grown under this program. InN was grown as an initial step towards growth of GaInN quantum wells. The InN growths were unsuccessful. Presumably the substrate temperature used was too high for this material. The nucleation of InN on sapphire did not occur similar to lack of nucleation of GaN when high temperatures were used. The lowest temperature attempted was 500°C. Lower temperatures may prove successful.

AlGaN was grown with ease. Al mole fractions were predicted based on calibrations from AlGaAs growths in the same machine. X-ray was used to determine Al content of AlGaN layers. The properties of AlGaN resemble those of GaN with simple shifts in energies corresponding to changes in bandgap. For example, PL (shown in Figure 16) of AlGaN is dominated by deep level emission which is shifted towards green wavelengths from yellow wavelengths seen for GaN. Si doping of AlGaN also resembles GaN characteristics. Single data points have been collected for Si doped AlGaN at concentrations of  $1 \times 10^{19} \text{ cm}^{-3}$  and  $5 \times 10^{19}$  with comparable mobilities to those for GaN.

The photoluminescence of AlGaN is affected similarly to GaN by doping. High n-type doping results in reduced defect emission and increased band edge emission. This observations support the deep level defect model

## **AlGaN PL**

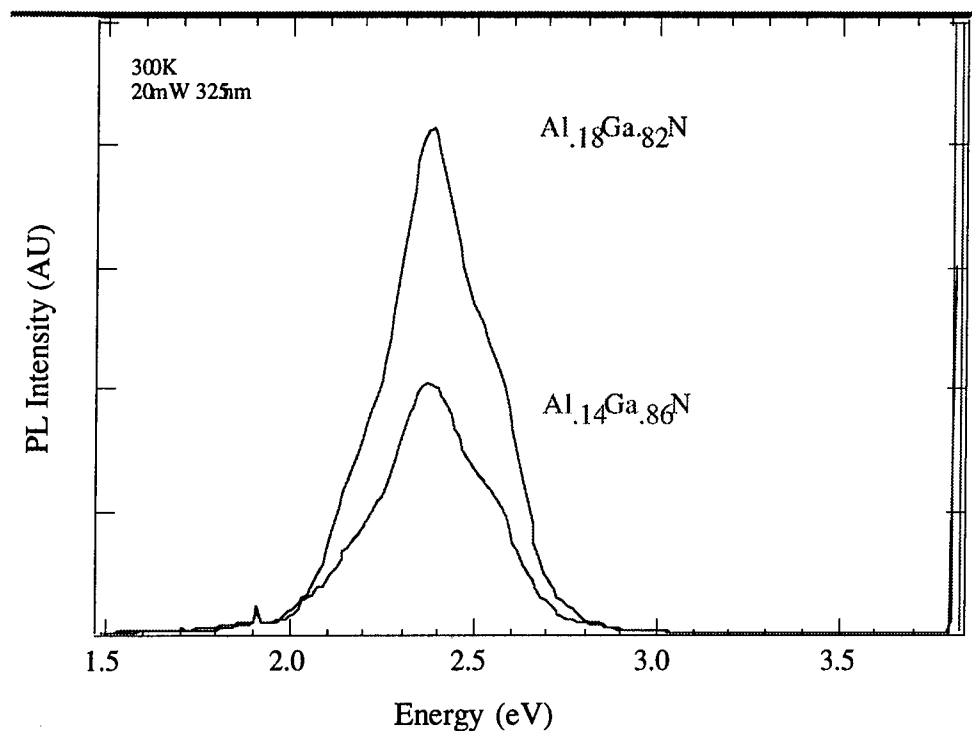


Figure 16 Room temperature PL from undoped AlGaN for two different compositions. No band edge luminescence is seen (the high energy signal is from the UV laser).

## Growth of cubic GaN by MBE

Some effort in this program was directed towards the growth of cubic GaN on cubic SiC. Since cubic GaN is a closer lattice match to cubic SiC, lower defect densities might be expected. There would be possible advantages for VCSEL applications using the cubic forms of GaN and AlGaN. The wavelength ranges available for this material system shown in Figure 1 provide a slightly different band of emission possibilities. The much larger lattice constant of cubic GaN might permit greater critical thicknesses than the Wurtzite form (critical thickness increases as the percentage of mismatch decreases). There is also some indication that electron mobilities might be higher in cubic GaN which would lead to even lower parasitic resistances.

## X-ray of cubic GaN

X-ray diffraction of cubic GaN grown on SiC is seen in Figure 17. The cubic peaks for cubic (002) and (004) GaN are clearly visible near the cubic SiC peaks. This result is very encouraging

as it shows GaN full width half-maximum values similar to those of the SiC substrate (which is itself grown on Si).

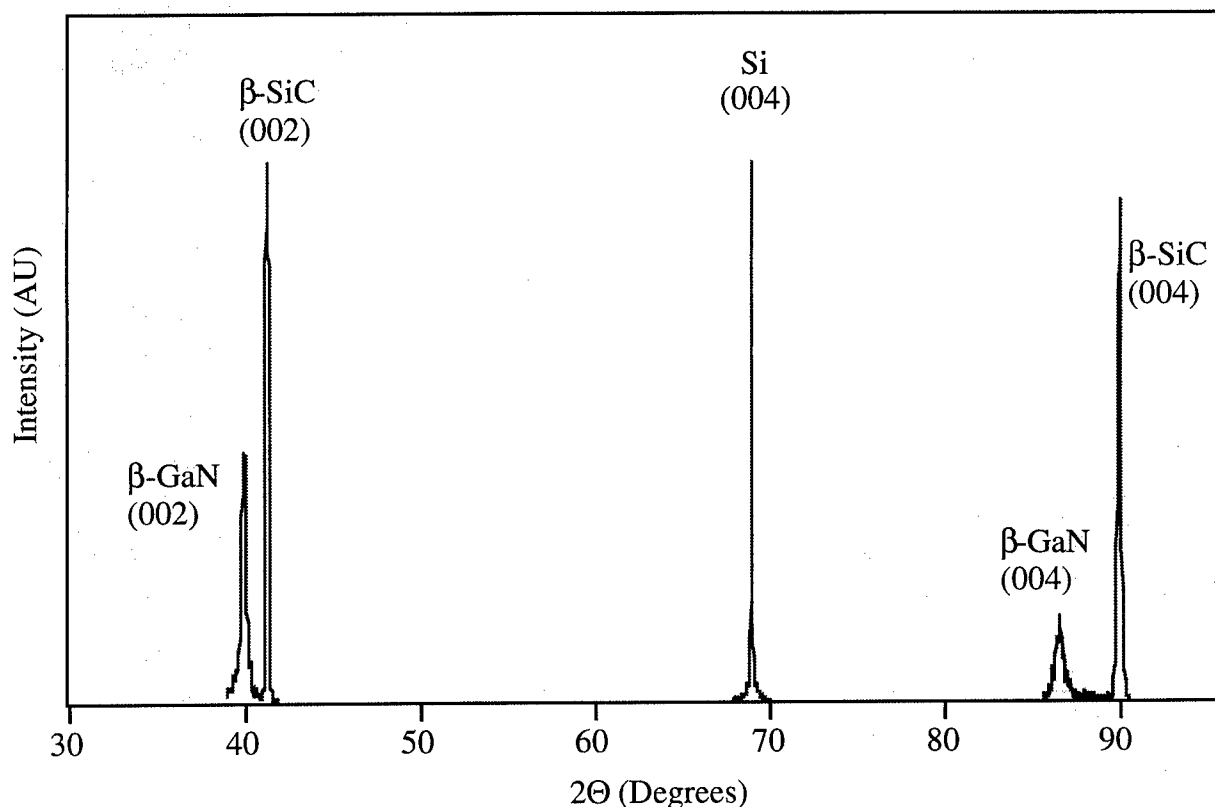


Figure 17 X-ray diffraction of 0.2μm thick cubic GaN grown on SiC at Cornell at 600W RF power

## Summary

The study of GaN VCSELs has focused almost exclusively on the development of the growth of GaN and AlGaIn by MBE. Much progress has been made in learning about the effects of growth conditions on electrical and optical properties of GaN. This first program has been successful in identifying the differences in approach required between growth of GaN and previous programs based on GaAs. Some fundamental techniques including indium-free mounting of metallized sapphire substrates, low temperature nucleation buffers, and even improving the reliability of the plasma RF source have been developed.

Electrical characterization of GaN shows the demonstration of exceptional n-type doping characteristics. N-type carrier concentrations of  $6 \times 10^{20} \text{ cm}^{-3}$  have been easily obtained for application to low resistance laser contacts. P-doping has been largely unsuccessful and will require future development. Undoped material with low conductivity has also been demonstrated.

The dominant materials difficulty which has been encountered has been the existence of significant defect densities arising from lattice mismatched growth of GaN on sapphire substrates. A model to understand the electrical and optical nature of the deep level arising from these defects has been developed. The only obvious solution to this problem is to employ GaN substrates which still have not been developed.

AlGaN appears to have similar properties to GaN and these materials should be able to be combined to form VCSEL structures providing careful attention is paid to critical thickness constraints. Some benefit might come from using cubic GaN and early growths of this material under this program has been successful.

## ***MISSION OF ROME LABORATORY***

Mission. The mission of Rome Laboratory is to advance the science and technologies of command, control, communications and intelligence and to transition them into systems to meet customer needs. To achieve this, Rome Lab:

- a. Conducts vigorous research, development and test programs in all applicable technologies;
- b. Transitions technology to current and future systems to improve operational capability, readiness, and supportability;
- c. Provides a full range of technical support to Air Force Material Command product centers and other Air Force organizations;
- d. Promotes transfer of technology to the private sector;
- e. Maintains leading edge technological expertise in the areas of surveillance, communications, command and control, intelligence, reliability science, electro-magnetic technology, photonics, signal processing, and computational science.

The thrust areas of technical competence include: Surveillance, Communications, Command and Control, Intelligence, Signal Processing, Computer Science and Technology, Electromagnetic Technology, Photonics and Reliability Sciences.